

REPORT DOCUMENTATION PAGE

Form Approved OMB NO. 0704-0188

The public reporting burden for this collection of information is estimated to average 1 hour per response, including the time for reviewing instructions, searching existing data sources, gathering and maintaining the data needed, and completing and reviewing the collection of information. Send comments regarding this burden estimate or any other aspect of this collection of information, including suggestions for reducing this burden, to Washington Headquarters Services, Directorate for Information Operations and Reports, 1215 Jefferson Davis Highway, Suite 1204, Arlington VA, 22202-4302. Respondents should be aware that notwithstanding any other provision of law, no person shall be subject to any penalty for failing to comply with a collection of information if it does not display a currently valid OMB control number.

PLEASE DO NOT RETURN YOUR FORM TO THE ABOVE ADDRESS.

1. REPORT DATE (DD-MM-YYYY)	2. REPORT TYPE	3. DATES COVERED (From - To)	
	New Reprint	-	
4. TITLE AND SUBTITLE Statistical Analysis of High-Cycle Fatigue Behavior of Friction Stir Welded AA5083-H321		5a. CONTRACT NUMBER W911NF-11-1-0207	5b. GRANT NUMBER
		5c. PROGRAM ELEMENT NUMBER 622105	5d. PROJECT NUMBER
6. AUTHORS M. Grujicic, G. Arakere, B. Pandurangan, A. Hariharan, C.-F. Yen, B. A. Cheeseman, C. Fountzoulas		5e. TASK NUMBER	5f. WORK UNIT NUMBER
7. PERFORMING ORGANIZATION NAMES AND ADDRESSES Clemson University Office of Sponsored Programs 300 Brackett Hall Clemson, SC 29634 -5702		8. PERFORMING ORGANIZATION REPORT NUMBER	
9. SPONSORING/MONITORING AGENCY NAME(S) AND ADDRESS(ES) U.S. Army Research Office P.O. Box 12211 Research Triangle Park, NC 27709-2211		10. SPONSOR/MONITOR'S ACRONYM(S) ARO 11. SPONSOR/MONITOR'S REPORT NUMBER(S) 57228-EG.5	
12. DISTRIBUTION AVAILABILITY STATEMENT Approved for public release; distribution is unlimited.			
13. SUPPLEMENTARY NOTES The views, opinions and/or findings contained in this report are those of the author(s) and should not be construed as an official Department of the Army position, policy or decision, unless so designated by other documentation.			
14. ABSTRACT A review of the literature revealed that high-cycle fatigue data associated with friction stir-welded (FSW) joints of AA5083-H321 (a solid-solution-strengthened and strain-hardened/stabilized Al-Mg-Mn alloy) are characterized by a relatively large statistical scatter. This scatter is closely related to the intrinsic variability of the FSW process and to the stochastic nature of the workpiece material microstructure/properties as well as to the surface condition of the weld. Consequently, the use of statistical methods and tools in the analysis of FSW			
15. SUBJECT TERMS AA5083, fatigue behavior, friction stir welding,maximum likelihood estimation			
16. SECURITY CLASSIFICATION OF: a. REPORT UU		17. LIMITATION OF ABSTRACT UU	18. NUMBER OF PAGES 19a. NAME OF RESPONSIBLE PERSON Mica Grujicic 19b. TELEPHONE NUMBER 864-656-5639

Report Title

Statistical Analysis of High-Cycle Fatigue Behavior of Friction Stir Welded AA5083-H321

ABSTRACT

A review of the literature revealed that high-cycle fatigue data associated with friction stir-welded (FSW) joints of AA5083-H321 (a solid-solution-strengthened and strain-hardened/stabilized Al-Mg-Mn alloy) are characterized by a relatively large statistical scatter. This scatter is closely related to the intrinsic variability of the FSW process and to the stochastic nature of the workpiece material microstructure/properties as well as to the surface condition of the weld. Consequently, the use of statistical methods and tools in the analysis of FSW joints is highly critical. A three-step FSW-joint fatigue-strength/life statistical-analysis procedure is proposed in this study. Within the first step, the type of the most appropriate probability distribution function is identified. The parameters of the selected probability distribution function, along with their confidence limits, are computed in the second step. In the third step, a procedure is developed for assessment of the statistical significance of the effect of the FSW process parameters and fatigue specimen surface conditions. The procedure is then applied to a set of stress-amplitude versus number of cycles to failure experimental data in which the tool translational speed was varied over four levels, while the fatigue specimen surface condition was varied over two levels. The results obtained showed that a two-parameter weibull distribution function with its scale factor being dependent on the stress amplitude is the most appropriate choice for the probability distribution function. In addition, it is found that, while the tool translational speed has a first-order effect on the AA5083-H321 FSW-joint fatigue strength/life, the effect of the fatigue specimen surface condition is less pronounced.

REPORT DOCUMENTATION PAGE (SF298)

(Continuation Sheet)

Continuation for Block 13

ARO Report Number 57228.5-EG
Statistical Analysis of High-Cycle Fatigue Behav ...

Block 13: Supplementary Note

© 2011 . Published in Journal of Materials Engineering and Performance, Vol. Ed. 0 20, (6) (2011), (, (6). DoD Components reserve a royalty-free, nonexclusive and irrevocable right to reproduce, publish, or otherwise use the work for Federal purposes, and to authroize others to do so (DODGARS §32.36). The views, opinions and/or findings contained in this report are those of the author(s) and should not be construed as an official Department of the Army position, policy or decision, unless so designated by other documentation.

Approved for public release; distribution is unlimited.

Statistical Analysis of High-Cycle Fatigue Behavior of Friction Stir Welded AA5083-H321

M. Grujicic, G. Arakere, B. Pandurangan, A. Hariharan, C.-F. Yen, B.A. Cheeseman, and C. Fountzoulas

(Submitted June 8, 2010)

A review of the literature revealed that high-cycle fatigue data associated with friction stir-welded (FSW) joints of AA5083-H321 (a solid-solution-strengthened and strain-hardened/stabilized Al-Mg-Mn alloy) are characterized by a relatively large statistical scatter. This scatter is closely related to the intrinsic variability of the FSW process and to the stochastic nature of the workpiece material microstructure/properties as well as to the surface condition of the weld. Consequently, the use of statistical methods and tools in the analysis of FSW joints is highly critical. A three-step FSW-joint fatigue-strength/life statistical-analysis procedure is proposed in this study. Within the first step, the type of the most appropriate probability distribution function is identified. The parameters of the selected probability distribution function, along with their confidence limits, are computed in the second step. In the third step, a procedure is developed for assessment of the statistical significance of the effect of the FSW process parameters and fatigue specimen surface conditions. The procedure is then applied to a set of stress-amplitude versus number of cycles to failure experimental data in which the tool translational speed was varied over four levels, while the fatigue specimen surface condition was varied over two levels. The results obtained showed that a two-parameter weibull distribution function with its scale factor being dependent on the stress amplitude is the most appropriate choice for the probability distribution function. In addition, it is found that, while the tool translational speed has a first-order effect on the AA5083-H321 FSW-joint fatigue strength/life, the effect of the fatigue specimen surface condition is less pronounced.

Keywords AA5083, fatigue behavior, friction stir welding, maximum likelihood estimation

1. Introduction

Friction stir welding (FSW) is a relatively new solid-state metal-joining process that was invented at The Welding Institute in the United Kingdom (Ref 1). FSW can be used to produce butt, corner, lap, T, spot, fillet, and hem joints, as well as to weld hollow objects, such as tanks and tubes/pipes, stock with different thicknesses, tapered sections, and parts with three-dimensional (3D) contours. This welding process is particularly suited for butt and lap joining of aluminum alloys which are otherwise quite difficult to join using conventional arc/fusion welding processes. FSW has established itself as a preferred joining technique for aluminum components, and its application for joining other *difficult-to-weld* metals is gradually expanding. Currently, this joining process is being widely used in many industrial

sectors such as shipbuilding/marine, aerospace, railway, land transportation, etc.

The basic concept behind the FSW process for the case of butt welding is displayed schematically in Fig. 1(a). Essentially, a non-consumable rotating tool, Fig. 1(b), consisting of a pin (usually conically shaped and containing threads, flutes, and flats) and a shoulder (usually containing scrolls or spirals) is forced to move along the contacting surfaces of two rigidly butt-clamped plates (the work-piece). Heat dissipation associated with frictional sliding at the shoulder/work-piece and pin/work-piece interfaces as well as the plastic deformation caused by the rotating and advancing tool causes the work-piece material to soften to a temperature near the respective solidus temperature. This, in turn, enables the tool to stir the surrounding material and cause its extrusion around the tool and its forging in the wake of the tool. Since, the tool is rotating as it traverses along the butted surfaces, the FSW process is essentially asymmetric, i.e., one typically makes a distinction between the so-called advancing side of the weld (the side on which the peripheral velocity of the rotating tool coincides with the transverse velocity of the tool) and the retreating side (the side on which the two velocities are aligned in the opposite directions).

Relative to the traditional fusion-welding technologies, FSW offers a number of advantages. Since a fairly detailed discussion pertaining to these advantages can be found in recent studies (Ref 2-4), a similar detailed account will not be given here. Instead, it should be noted that most of these advantages arise from the fact that FSW is associated with lower temperatures, does not involve fusion and re-solidification of the weld material, and that no filler metal, flux, or fuel/oxidizer is used.

M. Grujicic, G. Arakere, B. Pandurangan, and A. Hariharan, Department of Mechanical Engineering, Clemson University, Clemson, SC 29634; and **C.-F. Yen, B.A. Cheeseman, and C. Fountzoulas**, Army Research Laboratory, Survivability Materials Branch, Aberdeen Proving Ground, MD 21005-5069. Contact e-mails: mica.grujicic@ces.clemson.edu and gmica@clemson.edu.



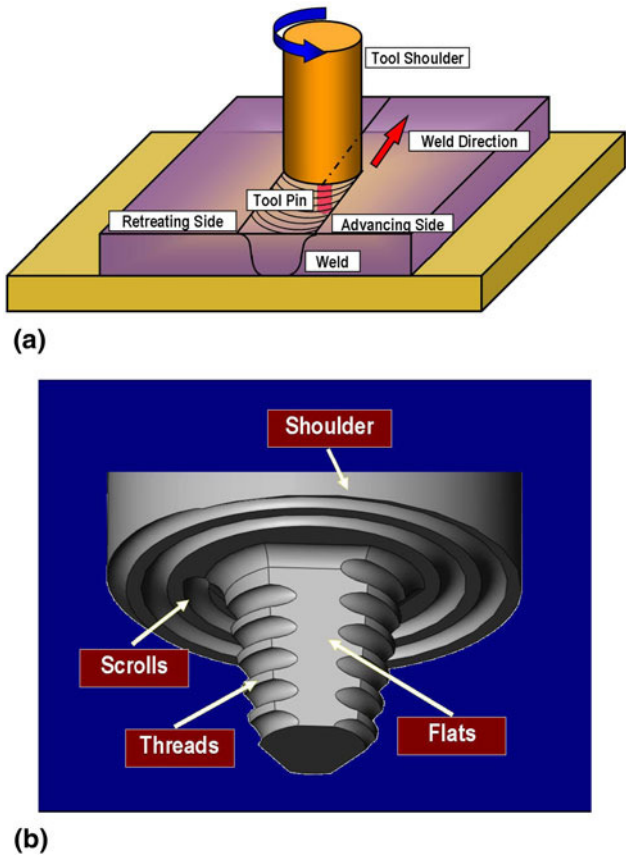


Fig. 1 (a) A schematic of the friction stir welding (FSW) process; and (b) a typical design of the FSW tool

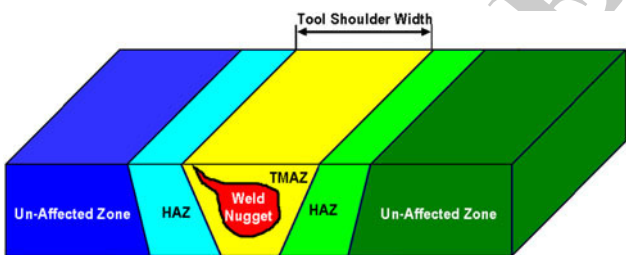


Fig. 2 A schematic of the four microstructural zones associated with the typical FSW joint

75 FSW normally involves complex interactions and competition
76 between various mass and heat transport phenomena,
77 plastic deformation and damage/fracture mechanisms, and
78 microstructure evolution processes (Ref 2-9). Consequently,
79 the material microstructure (and mechanical properties) in the
80 weld region are highly complex and spatially diverse. Metal-
81 lographic examinations of the Friction stir-welded (FSWed)
82 joints typically reveal the existence of the following four zones,
83 Fig. 2: (a) An unaffected (base-metal) zone which is far enough
84 from the weld so that material microstructure/properties are not
85 altered by the joining process; (b) The heat-affected zone
86 (HAZ) in which material microstructure/properties are effected
87 only by the thermal effects associated with FSW. While this
88 zone is normally found in the case of fusion welds, the nature of

the microstructural changes may be different in the FSW case due to generally lower temperatures and a more diffuse heat source; (c) The thermo-mechanically affected zone (TMAZ) which is located closer than the HAZ zone to the butting surfaces. Consequently, both the thermal and the mechanical aspects of the FSW affect the material microstructure/properties in this zone. Typically, the original grains are retained in this zone although they may have undergone severe plastic deformation; and (d) the weld nugget which is the innermost zone of an FSWed joint. As a result of the way the material is transported from the regions ahead of the tool to the wake regions behind the tool, this zone typically contains the so called onion-ring features. The material in this region has been subjected to most severe conditions of plastic deformation and high temperature exposure, and consequently contains a very fine dynamically recrystallized (equiaxed grain microstructure).

Despite the fact that FSW was discovered less than 20 years ago, this joining process has found a wide scale application in many industries. Among the most notable examples in which full advantage of the FSW process was taken to reduce production cost and fabricate durable structures are: (a) FSW is being used in a serial production of aluminum alloy-based ferryboat deck structures in Finland; (b) Al-Mg-Si-based alloy bullet-train cabins are commonly fabricated in Japan using FSW as the primary joining process; (c) Boeing predominantly utilizes FSW in the manufacture of Al-Cu-based rocket launch systems; (d) NASA has almost completely replaced conventional fusion welding processes with FSW for critical joints in the space-shuttle's external fuel-tanks which are manufactured using Al-Li-based alloy; and (e) General Electric has begun to use FSW in very demanding jet engine applications.

Recent efforts of the U.S. Army have been aimed at becoming more mobile, deployable, and sustainable while maintaining or surpassing the current levels of lethality and survivability. Current battlefield vehicles have reached in excess of 70 tons due to ever increasing lethality of ballistic threats which hinders their ability to be readily transported and sustained. Therefore, a number of research and development programs are under way to engineer light-weight, highly mobile, transportable, and lethal battlefield vehicles with a target weight under 20 tons. To attain these goals, significant advances are needed in the areas of light-weight structural- and armor-materials development (including aluminum-based structural/armor-grade materials).

Historically, aluminum alloy AA5083-H131 has been used in military-vehicle systems such as the M1113 and the M109, in accordance with the MIL-DTL-46027J specification (Ref 5). The main reasons for the selection of this alloy are its lighter weight, ease of joining by various welding techniques, a relatively high level of performance against fragmentation-based threats, and superior corrosion resistance. In recent years, FSW is being increasingly used during construction/fabrication of various military vehicle AA5083 welded structures (e.g., vehicle hulls). In previous studies (Ref 2-4), the effect of FSW process parameters on the blast/ballistic performance/survivability of such structures was discussed. It should be also recognized that in addition to meeting blast/ballistic survivability requirements, such structures should also meet (corrosion-based and fatigue-based) durability requirements. The main objective of this study is to address the issue of the effect of FSW and its process parameters on the fatigue behavior of AA5083-H321. Specifically, the issues regarding

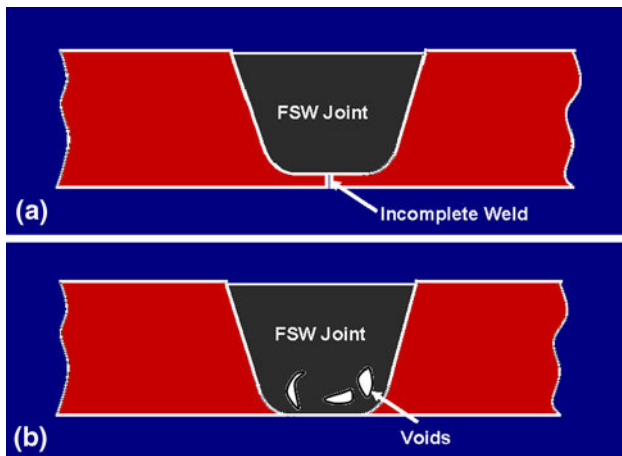


Fig. 3 Two most often observed FSW flaws: (a) incomplete welds; and (b) voids

152 the statistical analysis of the high-cycle fatigue results obtained
153 for AA5083-H321 FSW joints as described in Ref 6 are
154 discussed.

155 One of the main advantages of FSW over the traditional
156 fusion welding techniques is a significantly reduced defect
157 content within the weld. The two most common defects found
158 within the FSW joints are: (a) lack of penetration (caused by an
159 insufficient length of the tool pin), Fig. 3(a); and (b) voids and
160 root defects (also known as kissing bonds), Fig. 3(b). While the
161 former defects can be readily eliminated by properly designing
162 the FSW tool, the true origin for the latter type of defects is not
163 well understood and/hence/they are more challenging to deal
164 with. To make the situation worse, these defects are generally
165 difficult to detect using conventional techniques like radiography
166 and ultrasonics (Ref 7), since they can occur in any
167 orientation. The presence and the concentration of these defects
168 is affected both by the type of the alloys being welded and by
169 the FSW process parameters, while they generally profoundly
170 affect fatigue strength/life of the welded joints (Ref 6). Due to
171 stochastic nature of the void/root-defect generation process
172 (e.g., the material flow underneath the tool-shoulder on the
173 advancing side is often of a chaotic nature and is associated
174 with singularities which may lead to the formation of defects),
175 the resulting fatigue strength/life data typically show a
176 relatively wide distribution and, hence, they must be analyzed
177 using statistical tools. An example of such a statistical analysis
178 of the AA5083-H321 high-cycle fatigue results (Ref 6) is
179 presented in this study.

180 The organization of the article is as follows: A summary of
181 the high-cycle fatigue experimental testing procedure used and
182 the experimental results obtained in Ref 6 for the case AA5083-
183 H321 FSW-joints is presented in section 2.1. A new three step
184 statistical-analysis procedure is introduced in section 2.2. The
185 application of this procedure to the AA5083-H321 FSW-joint
186 high-cycle fatigue data as reported in Ref 6 is carried out in
187 section 3. Specifically, in section 3.1, the optimal type of the
188 probability distribution function is identified. Determination of
189 the most-likely estimates for the selected probability-distribution
190 function is carried out in section 3.2. Statistical significance
191 of the effect of the two controlled variates (the tool
192 translational speed and the fatigue specimen surface condition)
193 is assessed in section 3.3. A brief summary of the study carried

out and the conclusions resulting from this study are presented
in section 4.

2. Analyses and Procedures

2.1 High-Cycle Fatigue Results from Ref 6

196 As mentioned earlier, the main objective of this study is to
197 introduce and apply a statistical analysis to the AA5083-H321
198 high-cycle fatigue results reported in Ref 6. In this section, a
199 brief description is provided regarding the details of the FSW
200 joining process and of the high-cycle fatigue strength/life
201 experimental assessment procedure.

202 The as-rolled AA5083-H321 plates of dimensions: $L \times$
203 $W \times H$ (1000 mm \times 500 mm \times 8 mm) were used in the exper-
204 iment described in Ref 6. Two such plates were welded at a
205 time to form a FSWed workpiece from which the fatigue
206 specimens were machined. Chemical and mechanical property
207 characterizations of the base material yielded the following
208 results: 4.20 wt.% Mg, 0.60 wt.% Mn, 0.25 wt.% Si, 0.15 wt.%
209 Fe, 0.09% Cr and 0.09% Zn; yield strength = 264 MPa and
210 Ultimate Tensile Strength = 350 MPa. The H321 temper
211 designation denotes a strain-hardened and stabilized condition
212 of the alloy with the final strength level corresponding to
213 roughly a quarter of that observed in the material before the
214 stabilization heat treatment. Typically, the yield strength of the
215 FSW joint material is circa 160 MPa (i.e., around 40% lower
216 than that in the base metal).

217 The FSW tool used was made of tool steel, had a 25 mm-
218 diameter shoulder and a 10 mm diameter 7.9 mm length pin.
219 The tool rotational speed was kept constant at a value of
220 500 rpm while four different (80, 95, 130, and 200 mm/min)
221 tool translational speeds were used. The tool was tilted by 2.5°
222 in the direction of travel, and had a plunge depth of 0.2 mm.
223 Rectangular section, hourglass-shaped fatigue specimens were
224 machined from the FSWed workpieces. Gauge length and
225 width of the fatigue specimens were 40 and 16 mm, respec-
226 tively, while the gage thickness was kept as close as possible to
227 the original 8 mm plate thickness. Fatigue (cyclic loading)
228 testing was done at a frequency of 112 Hz in the fully reversed
229 uniaxial loading mode with the (algebraically) lowest stress to
230 (algebraically) highest stress ratio = -1.0.

231 In addition to investigating the effect of tool translational
232 velocity on the fatigue strength/life of the AA5083-H321 FSW
233 joints, the effect of the fatigue-sample surface condition was
234 also studied. Specifically, two types of surface conditions were
235 considered: (a) the so-called as-welded condition in which
236 small burrs at the edges of the weld region were removed while
237 ~0.2-mm-high tool shoulder ledges were left; and (b) the
238 so-called polished condition in which both burrs at the edges
239 and the tool shoulder ledges were removed leaving a fatigue
240 sample with smooth surfaces and free of stress concentrators.
241 This portion of the study enabled separate assessment of the
242 relative contributions of surface and interior defects to the
243 fatigue strength/life of FSWed joints.

244 A summary of the high-cycle fatigue strength/life results for
245 the as-welded and polished conditions of the specimen surface
246 are displayed in Fig. 4(a) and (b), respectively. In each figure,
247 stress amplitude versus number of cycles to failure results are
248 presented at four different tool translational speeds. A quick
249 examination of the results displayed in these figures shows
250



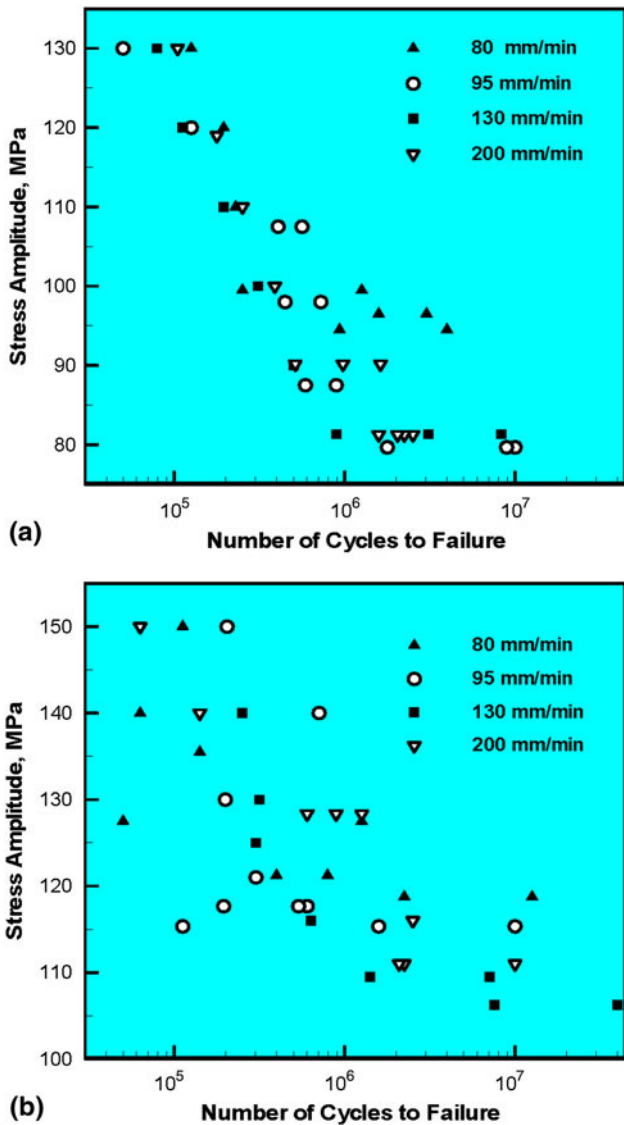


Fig. 4 Stress amplitude vs. number of cycles to failure results for AA5083-H321 FSW joints at four different tool translational speeds and for two fatigue-specimen surface conditions: (a) as-welded; and (b) polished

252 (a) significant spread in the number of cycles to failure at
253 nominally identical FSW-processing, specimen-surface and
254 fatigue-testing conditions; and (b) a generally larger value of
255 the number of cycles to failure for the case of polished fatigued
256 samples.

2.2 Statistical Analysis of the FSW-Joint Fatigue Results

258 In this section, a simple statistics-based analysis is described
259 which would be used to address the issue of the spread in the
260 FSW-joint fatigue results associated with the stochastic nature
261 of the location, orientation, and size of the welding-induced
262 defects. The proposed procedure is depicted, in Fig. 5, using a
263 flow chart type of diagram. As seen, the first step in this
264 procedure is the identification of the appropriate probability
265 distribution function which best accounts for the observed
266 spread in the results. This is typically accomplished using the
267 so-called “chi-square goodness of fit” method (Ref 8). Once

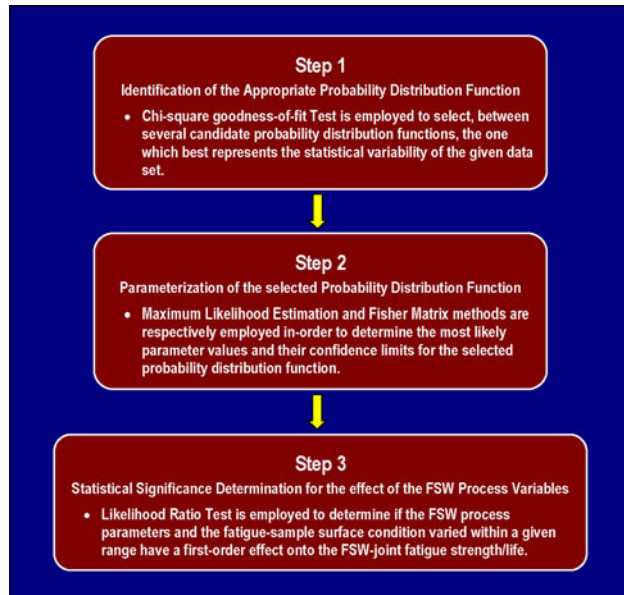


Fig. 5 A flow chart of the proposed three-step procedure for statistical analysis of FSW joint fatigue data

268 the type of the appropriate probability density function is
269 identified, the so-called maximum likelihood estimation (MLE)
270 procedure (Ref 9) is invoked to obtain the optimal estimates for
271 the probability density function parameters and their respective
272 ranges for a given statistical level of confidence. The informa-
273 tion obtained at this point is sufficient, at a given level of
274 confidence, to enable the determination of the fatigue life at a
275 prescribed level of the service stress or determination of the
276 maximum allowable surface stress which guarantees the desired
277 fatigue life. Finally, one can investigate the magnitude of the
278 effect of the FSW process parameters and fatigue-sample
279 surface condition, in a statistical sense, on the fatigue strength/
280 life of the FSW joints. This is typically done using the so-called
281 likelihood ratio method (Ref 10). In the remaining subsections
282 of this section, a brief description is provided for the three
283 statistical-analytical tools identified above, i.e., the chi-square
284 goodness of fit method, the MLE method, and the likelihood
285 ratio method.

286 **2.2.1 Chi-Square Goodness of Fit.** As mentioned earlier,
287 the chi-square goodness of fit test (Ref 8), is used to identify the
288 appropriate type of probability distribution function for a given
289 set of data. This method can be applied to any univariate
290 distribution for which the cumulative distribution function can
291 be calculated. Before the method could be applied, the data
292 have to be binned, i.e., grouped into classes. Once this is done,
293 the mean and the standard deviation for the bin data can be
294 calculated and, for a given type of the probability, the values of
295 the cumulative density function evaluated at the variate levels
296 corresponding to the bin edges. Then, for a given bin, a product
297 of the total number of data points and the positive difference in
298 the cumulative distribution function values at the two edges of
299 the bin are used to calculate the expected number of
300 observations in a given bin, E_i ($i = 1, \dots, \text{number of bins}(N)$). The
301 corresponding experimental observations are denoted as
302 O_i . To assess the appropriateness of the given distribution, the
303 following null hypothesis is formulated:

304 H_0 The experimental data follow the assumed distribution.



306
307

To test this hypothesis, the following chi-square test statistic is defined:

$$\chi^2 = \sum_{i=1}^N (O_i - E_i)^2 / E_i \quad (\text{Eq 1})$$

The test statistic follows, approximately, a chi-square distribution with $(k - c)$ degrees of freedom, where, k is the number of non-empty bins, and c is the number of parameters in the assumed probability function plus one. The null hypothesis given above is rejected, at the confidence level of $(1 - \alpha)$ when the following condition is satisfied:

$$\chi^2 > \chi^2_{(\alpha, k-c)} \quad (\text{Eq 2})$$

where $\chi^2_{(\alpha, k-c)}$, corresponds to the test-statistic evaluated at $(k - c)$ degrees of freedom chi-square cumulative distribution function value of $(1 - \alpha)$. To aid in the understanding of this procedure, the case of a chi-squared distribution function for a three degrees-of-freedom and at a confidence level of $(1 - \alpha) = 0.95$ is depicted in Fig. 6(a) and (b).

The aforementioned procedure can be used to determine whether the chosen probability function accounts well for the given set of data. On the other hand, when two or more probabilities are found to be appropriate for a given set of data, the one associated with the lowest value of the test statistic is considered the most appropriate.

2.2.2 Maximum Likelihood Estimation. Maximum likelihood estimation (MLE) is a common statistical method used for fitting a pre-selected type of the probability density function (PDF) to a given set of data, and for providing the estimates for the function parameters. The basic idea behind the MLE method is that, for a given type of PDF, it computes the values of function parameters which maximize the likelihood that the given set of data belongs to the population PDF associated with these parameters. Toward that end, a likelihood function is defined in terms of the preselected-PDF with yet-undetermined parameters. The function is next maximized with respect to the unknown parameters resulting in their “*most likely*” estimates.

In this study, the likelihood function, L , is defined as

$$\ln[L] = \sum_{i=1}^R \ln[f(N_i, p_1, p_2, \dots)] + \sum_{j=1}^U \ln[1 - F(S_j, p_1, p_2, \dots)] \quad (\text{Eq 3})$$

where f and F are the failure probability density function (PDF) and cumulative distribution function (CDF), respectively, R is the number of failed specimens, U is the number of survived specimens, N_i is the number of cycles at failure for the i th specimen, S_j is the number of cycles at which the unfailed j th specimen test was suspended, and p_1, p_2, \dots are the unknown parameters in f and F .

The MLE method described above yields the most likely values of the parameters for the assumed probability density function. However, these parameters themselves are statistical variables and in the limit of a large sample size they are distributed in accordance with the normal distribution function. Consequently, in-order to assess the error associated with the computed value of the likelihood function, one needs to know the confidence limits for each of the parameters (i.e. the range for each parameter associated with a given level of statistical confidence). To determine these confidence limits, one can

employ the so-called Fisher Matrix method (Ref 11). In the remainder of this section, some of the details of the Fisher Matrix method for the case of a two-parameter weibull distribution function is provided. The two parameters are commonly referred to as the scale factor θ and shape factor. Following the procedure outlined in Ref 11, the confidence limits at a confidence level of $(1 - \alpha)$ for these two parameters can be calculated as follows:

$$\beta_U = \hat{\beta} e^{\frac{K_2 \sqrt{\text{Var}(\hat{\beta})}}{\hat{\beta}}} \quad (\text{Eq 4})$$

$$\beta_L = \frac{\hat{\beta}}{e^{\frac{K_2 \sqrt{\text{Var}(\hat{\beta})}}{\hat{\beta}}}} \quad (\text{Eq 5})$$

$$\eta_U = \hat{\eta} e^{\frac{K_2 \sqrt{\text{Var}(\hat{\eta})}}{\hat{\eta}}} \quad (\text{Eq 6})$$

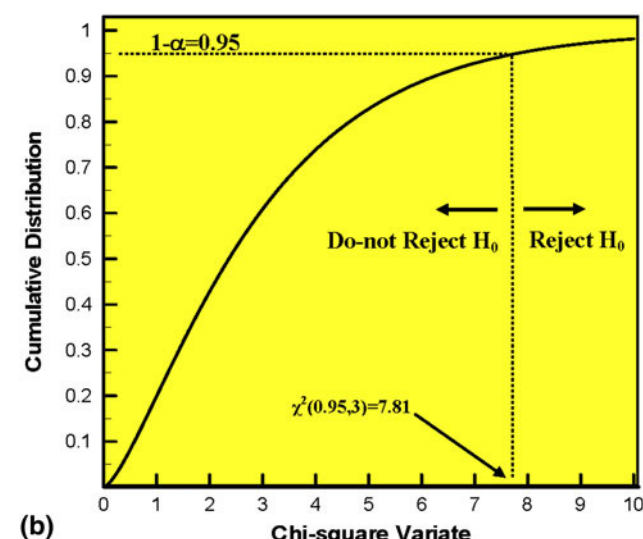
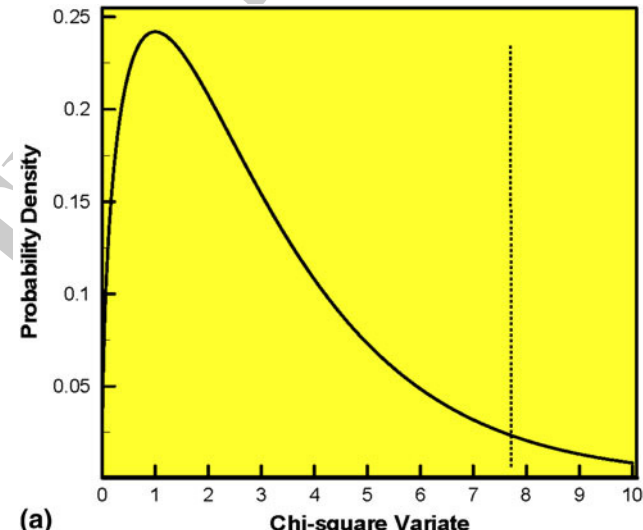


Fig. 6 Three degree-of-freedom chi-squared: (a) probability density; and (b) cumulative distribution functions used for testing the hypothesis H_0 at a confidence level of $(1 - \alpha) = 0.95$

361
362
363
364
365
366
367
368

370

372

374

375 $\eta_L = \frac{\hat{\eta}}{e^{\frac{K_\alpha \sqrt{\text{Var}(\hat{\eta})}}{\eta}}}$ (Eq 7)

377 where K_α is implicitly defined by

$$\alpha = \frac{1}{\sqrt{2\pi}} \int_{K_\alpha}^{\infty} e^{-\frac{t^2}{2}} dt = 1 - \phi(K_\alpha) \quad (\text{Eq 8})$$

389 To determine variances and covariances of the two parameters,
381 the value of the local inverse fisher matrix is calculated as
382 follows:

$$\begin{pmatrix} \text{Var}(\hat{\beta}) & \text{Cov}(\hat{\beta}, \hat{\eta}) \\ \text{Cov}(\hat{\beta}, \hat{\eta}) & \text{Var}(\hat{\eta}) \end{pmatrix} = \begin{pmatrix} -\partial^2 \ln(L)/\partial \beta^2 & -\partial^2 \ln(L)/\partial \beta \partial \eta \\ -\partial^2 \ln(L)/\partial \beta \partial \eta & -\partial^2 \ln(L)/\partial \eta^2 \end{pmatrix}^{-1}$$

$$\beta = \hat{\beta}, \eta = \hat{\eta} \quad (\text{Eq 9})$$

384 To compute the second-order partial derivatives appearing in
386 Eq 9, the chain rule has to be applied (e.g., $-\partial^2 \ln(L)/\partial \beta^2 = -\partial^2 \ln(L)/\partial f^2 * \partial f^2/\partial \beta^2$), since, the two parameters are
387 functionally related to f , while, f is functionally related to
388 L . Mathematical expressions for the weibull probability density,
389 f , and cumulative distribution functions, F , are given later in
390 this document.

392 **2.2.3 Likelihood Ratio Method.** When two or more data
393 sets are each analyzed using the MLE method and the
394 corresponding parameter-estimate and likelihood-function values
395 computed, the likelihood ratio method can be used to
396 determine whether the data are associated with the same
397 population. In this study, this method is employed to determine
398 if the variations in the FSW process parameters, and the fatigue
399 specimen surface conditions impart a statistically significant
400 effect to the fatigue strength/life of the FSW joints. Toward that
401 end, the null hypothesis is formulated as

402 **H₀** The fatigue strength/life data obtained under different
403 combinations of the FSW process parameters and fatigue-
404 specimen surface conditions are all associated with the same
405 population.

406 In this case, the test statistic is defined as

$$T = 2 \left[\sum_{i=1}^K (\ln(L_i) - \ln(L_p)) \right] \quad (\text{Eq 10})$$

408 where K is the total number of different data sets, L_i is the
409 maximum likelihood for the i th sample and L_p is the
410 maximum likelihood for the pooled data. The data pool is
411 obtained by combining all K data sets into a single data set
412 and by applying the MLE method to it. Since the test statistic
413 is again assumed to follow a chi-square distribution function,
414 the procedure analogous to that employed in the chi-square
415 goodness of fit method is utilized. In other words, if the com-
416 puted test statistic is larger than its counter part associated
417 with the value of chi-square cumulative distribution function
418 (with the number of degrees of freedom equal to the number
419 of parameters in the PDF) of $(1 - \alpha)$, then the null hypothesis
420 is rejected at the confidence level of $(1 - \alpha)$.

3. Results and Discussion

In this section, the results of the statistical analysis of the fatigue strength/life data as reported in Ref 6 are presented and discussed. The section is organized in such a way that it fully complies with the three-step procedure depicted in Fig. 5.

3.1 Identification of the Appropriate Probability Distribution Function

In accordance with the three-step procedure depicted in Fig. 5, the first task is to employ the chi-square goodness of fit method in-order to identify the appropriate type of the probability distribution function which best represents the statistical variation in the given data set. Unfortunately, the chi-square goodness of fit method requires a relatively large data set which was not available in this study. To overcome this problem, it was assumed that the same type of probability distribution function identified as appropriate in other alloy systems will also be appropriate in the case of AA5083-H321. Specifically, in Ref 12, it was demonstrated that a two parameter weibull distribution function is the appropriate choice for the case of the fatigue strength/life data for many metallic systems. Consequently, this type of distribution function was adopted in this study.

An examination of the results displayed in Fig. 4(a) and (b) revealed that at a given stress-amplitude and for a given combination of the tool translational speed and the fatigue-specimen surface condition, the data set is way too small to carry-out any meaningful statistical analysis. To overcome this problem, and in accordance with the suggestions presented in Ref 12, the natural logarithm of the scaling parameter, $\ln(\theta)$, in the weibull distribution function is assumed to be a linear function of the stress-amplitude, σ , as

$$\ln(\theta) = C_1 + C_2 \sigma \quad (\text{Eq 11})$$

while, the shape parameter, β , is defined as

$$\beta = e^{D_1} \quad (\text{Eq 12})$$

where C_1 , C_2 , and D_1 are the unknown coefficients/parameters. This procedure increased the number of parameters in the weibull distribution to three but enabled the data associated with different stress amplitudes, at the same combination of the tool translational speed and the fatigue specimen surface condition, to be combined into a single data set. This, in-turn, enabled us to provide a more meaningful statistical analysis of the fatigue strength/life data.

The weibull probability density and the cumulative distribution functions in-terms of the two original parameters θ and β are defined, respectively, as

$$f(N) = \frac{\beta}{\theta} \left(\frac{N}{\theta} \right)^{\beta-1} e^{-\left(\frac{N}{\theta} \right)^\beta} \quad (\text{Eq 13})$$

and

$$F(N) = 1 - e^{-\left(\frac{N}{\theta} \right)^\beta} \quad (\text{Eq 14})$$

where the variate N in this case denotes the number of cycles to failure.

An example of the effect of the values of the scale and shape parameters on the weibull probability density and cumulative



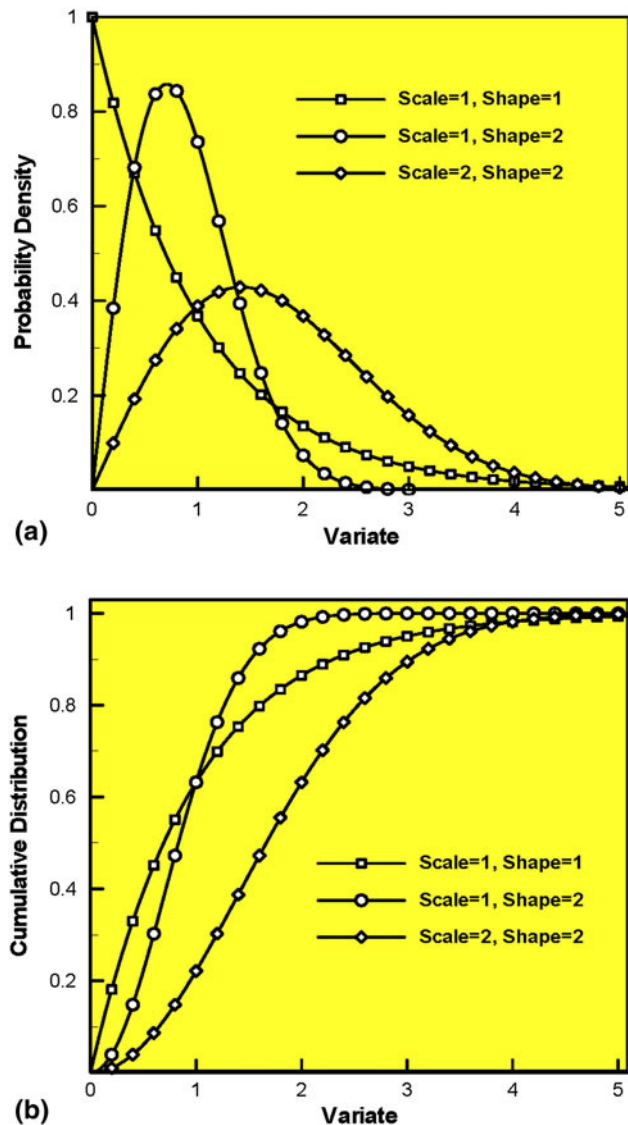


Fig. 7 The effect of the scale and shape parameters on the weibull: (a) probability density; and (b) cumulative distribution functions

distribution functions is displayed in Fig. 7(a) and (b). It is seen, that at a constant value of the shape parameter, an increase in the scale parameter value stretches the PDF curve in the horizontal direction. This will also cause a reduction in the peak value of the PDF, since the area under the PDF curve is constant and equal to one. As far as the effect of the shape parameter is concerned, it is seen that it could be quite large, markedly changing the shape of the PDF curve.

3.2 Estimation of the Weibull Distribution Parameters and their Confidence Limits

In the previous section, it was established that a two-parameter weibull distribution function with a stress-dependent scale parameter is the appropriate choice for the statistical analysis of the fatigue strength/life data considered. In this section, the MLE method is employed to determine the values of these parameters and their confidence limits. As discussed in the previous section, stress dependency of the scale parameter makes the weibull distribution effectively a three-parameter function.

The results of the MLE analyses for the four tool translational speeds (80, 95, 130, and 200 mm/min) and the as-welded surface condition for the fatigue specimens are summarized in Table 1. The corresponding MLE results for the case of the polished surface condition for the fatigue specimens are summarized in Table 2. These results are used in the remainder of this section to show the relationship between the fatigue strength and fatigue life at a given confidence level. In addition, these results will be used in the next section to assess the magnitude of the effect of the tool translational speed and the fatigue-specimen surface condition on the fatigue strength/life of the FSW joints.

An example of the resulting stress amplitude and the number of cycles to failure-dependent probability density function for the case of the tool translational speed of 80 mm/min and as-welded surface condition of the fatigue sample is depicted in Fig. 8. The results displayed in this figure clearly show that, as expected, the peak in the probability density curve moves toward a lower number of cycles to failure as stress amplitude is increased. At the same time, the distribution variance is reduced, while the peak value is increased. The practical

Table 1 The results of the maximum likelihood estimation (MLE) analyses for the fatigue strength/life data of AA5083-H321 FSWed joints and for an as-welded surface condition of the fatigue samples

Tool speed, mm/min		C_1	C_2	D_1	$\ln(L)$
80	Most likely	10.5490	Most likely	-0.004	1.3772
	Lower bound	9.9055	Lower bound	-0.0038	1.2932
	Upper bound	11.1925	Upper bound	-0.0042	1.4612
	Most likely	5.8359	Most likely	-0.0071	1.5015
95	Lower bound	5.4799	Lower bound	-0.0067	1.4099
	Upper bound	6.1919	Upper bound	-0.0075	1.5931
	Most likely	11.6037	Most likely	-0.0141	1.5149
	Lower bound	10.8959	Lower bound	-0.0132	1.4225
130	Upper bound	12.3115	Upper bound	-0.015	1.6073
	Most likely	12.4741	Most likely	-0.0458	1.4329
	Lower bound	11.7132	Lower bound	-0.043	1.3455
	Upper bound	13.235	Upper bound	-0.0486	1.5203
C ₂ has units of MPa ⁻¹ ; confidence level = 0.95					

C₂ has units of MPa⁻¹; confidence level = 0.95



Table 2 The results of the maximum likelihood estimation (MLE) analyses for the fatigue strength/life data of AA5083-H321 FSWed joints and a polished surface condition of the fatigue samples

Tool speed, mm/min		C_1		C_2		D_1	$\ln(L)$
80	Most likely	11.5239	Most likely	-0.0451	Most likely	1.2364	2.0337
	Lower bound	10.8209	Lower bound	-0.0423	Lower bound	1.1610	
	Upper bound	12.2269	Upper bound	-0.0479	Upper bound	1.3118	
95	Most likely	12.6252	Most likely	-0.0883	Most likely	0.1730	2.5888
	Lower bound	11.8551	Lower bound	-0.0829	Lower bound	0.1624	
	Upper bound	13.3953	Upper bound	-0.0937	Upper bound	0.1836	
130	Most likely	5.7619	Most likely	-0.0406	Most likely	1.36	2.3746
	Lower bound	5.4104	Lower bound	-0.0381	Lower bound	1.277	
	Upper bound	6.1134	Upper bound	-0.0431	Upper bound	1.4430	
200	Most likely	10.1239	Most likely	-0.0471	Most likely	1.2412	2.4922
	Lower bound	9.5063	Lower bound	-0.0442	Lower bound	1.1655	
	Upper bound	10.7415	Upper bound	-0.05	Upper bound	1.3169	

C_2 has units of MPa⁻¹; confidence level = 0.95

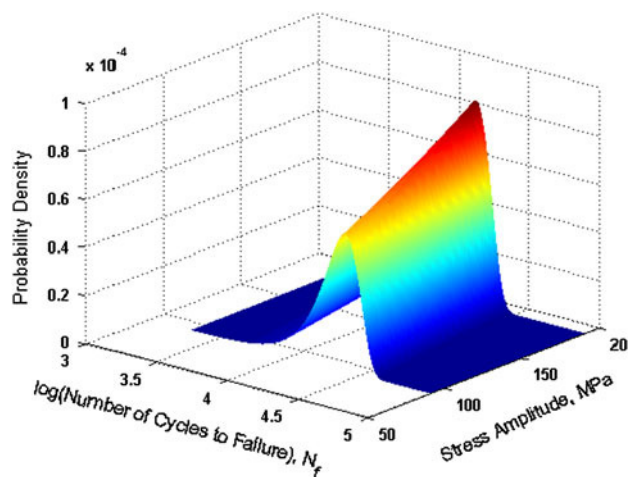


Fig. 8 Stress amplitude and number of cycles to failure-dependent probability density function for the case of the tool translational speed of 80 mm/min and as-welded surface condition of the fatigue sample

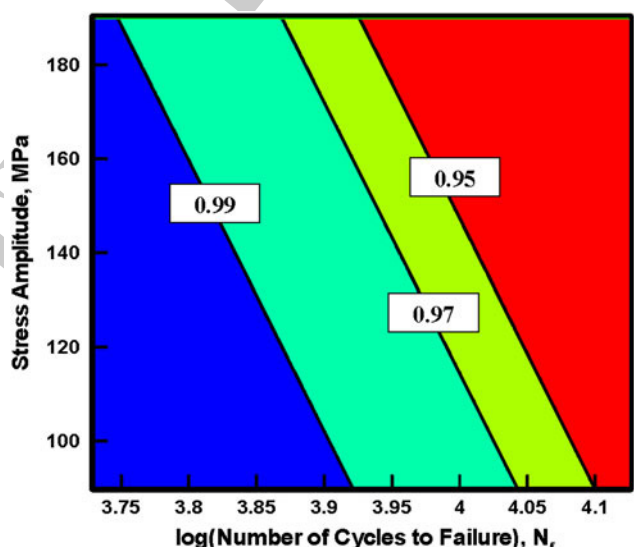


Fig. 9 Trade-off between the fatigue strength (as represented by the stress amplitude) and the fatigue life (as represented by the number of cycles to failure) at three different levels of the statistical confidence for the case of tool translational speed of 80 mm/min and as-welded surface condition of the fatigue sample

514 significance of these changes in the probability density function
515 is discussed below.

516 The functional relationship between the fatigue strength
517 (as represented by the stress amplitude) and the fatigue life
518 (as represented by the number of cycles to failure) at a given
519 confidence level is demonstrated using a contour plot as shown
520 in Fig. 9. For the case of a 80 mm/min tool translational speed
521 and the as-welded surface condition of the fatigue specimen,
522 the confidence levels indicated in this figure are computed as
523 $(1 - F)$, where F is the corresponding weibull cumulative
524 distribution function. The results displayed in Fig. 9 show that
525 (a) at a given level of confidence, higher fatigue strength is
526 associated with a lower level of fatigue life; and (b) at a
527 constant fatigue-strength level, a longer fatigue life can be
528 obtained at the expense of a reduction in the statistical
529 confidence. Alternatively, at a given fatigue-life level, higher
530 fatigue strengths can be expected only if the level of statistical
531 confidence is reduced.

3.3 Statistical Significance of the Effects of FSW Process and Specimen Surface Condition

In this section, the results displayed in Table 1 and 2 are combined with additional pooled samples' MLE results and used within the Likelihood Ratio method to determine the statistical significance of the FSW tool translational speed and the fatigue-specimen surface condition on the fatigue strength/life of the FSW joints. Specifically, the following two questions were addressed: (a) Do the variations in the tool translational speed in a 80-200 mm/min range have a statistically significant effect on the materials fatigue strength/life when the surface condition of the fatigue specimen is kept constant? and (b) Does the variation of the fatigue specimen surface condition at a constant tool translational speed have a statistically significant effect on the materials fatigue strength/life?

532
533
534
535
536
537
538
539
540
541
542
543
544
545
546

547 **3.3.1 The Effect of Tool Translational Speed.** The null-
 548 hypothesis in this case is defined as:

549 **H₀** The variation of tool translational speed in an 80-
 550 200 mm/min range does not have a statistically significant
 551 effect on the FSW-joint fatigue strength/life. In other words, at
 552 the same surface condition of the fatigue specimens, the data
 553 sets associated with different values of the tool translational
 554 speed belong to the same population.

555 To test this hypothesis, the following test statistic is defined

$$T = 2 \left[\sum_{i=1}^K (\ln(L_i) - \ln(L_{\text{Pool}})) \right] \quad (\text{Eq 15})$$

557 where the number of data sets, $K(=4)$, is equal to the number
 558 of tool-translational velocities at the same fatigue specimen
 559 surface condition. The maximum likelihood function for the
 560 pooled data set is obtained by combining all the data sets at
 561 the same fatigue-specimen surface condition into a single data
 562 set and by performing the MLE analysis on it.

563 The results of the aforementioned procedure are summarized
 564 in Table 3. It is seen that the T -statistic values for the as-
 565 welded and the polished surface conditions are 20.72 and
 566 24.23, respectively. To determine if the null hypothesis defined
 567 earlier in this section should be rejected, these T -statistic values
 568 should be compared with the chi-square value associated with
 569 the given number of degrees of freedom and a statistical
 570 confidence level. In this case, a chi-square distribution function
 571 associated with the number of degrees of freedom equal to the
 572 number of weibull distribution function parameters ($=3$) is
 573 used. For this chi-square distribution function, the critical
 574 chi-square value associated with a 0.95 confidence level is
 575 computed as, $\chi_{(0.05,3)}^2(=7.81)$. When employing the procedure
 576 described in section 2.2, it is found that the null hypothesis
 577 should be rejected for both surface conditions of the fatigue
 578 specimen. This finding is simply based on the fact that both
 579 T values mentioned earlier in this section are greater than 7.81.
 580 To summarize, the results obtained in this section simply
 581 suggest that a variation of the tool translational speed in a
 582 80-200 mm/min range gives rise to the changes in the weld
 583 microstructure, defect content, and properties, which are
 584 reflected in first-order changes of the FSW joint fatigue
 585 strength/life.

586 **3.3.2 The Effect of the Fatigue Specimen Surface 587 Condition.** The null-hypothesis in this case is defined as

588 **H₀** The variation of the fatigue specimen surface condition at
 589 a constant tool translational speed does not have a statistically
 590 significant effect on the FSW-joint fatigue strength/life. In other
 591 words, at the same tool translational speed, the data sets
 592 associated with the two fatigue specimen surface conditions
 593 belong to the same population.

594 To test this hypothesis, a procedure analogous to the one
 595 presented in the previous section is employed. The test statistic
 596 used in this case is also defined by Eq 15, but the number of
 597 data sets K is equal to two. That is, the pooled data set in this
 598 case is obtained by combining two data sets associated with the
 599 same value of the tool translational speed but having different
 600 fatigue specimen surface conditions. As a consequence, the
 601 procedure yielded four T values, one for each of the four tool
 602 translational speeds.

**Table 3 The results of the likelihood ratio analyses
 of the effect of the tool translational speed on the fatigue
 strength/life of AA5083-H321 FSWed joints for the
 as-welded and polished surface conditions**

Fatigue samples surface condition	T-statistic	Conclusion
As-welded	20.72	Since $20.72 > \chi_{(0.05,3)}^2(=7.81)$, reject the null-hypothesis
Polished	24.23	Since $24.23 > \chi_{(0.05,3)}^2(=7.81)$, reject the null-hypothesis

**Table 4 The results of the likelihood ratio analyses
 of the effect of the fatigue-specimen surface condition
 on the fatigue strength/life of AA5083-H321 FSWed joints
 for four tool translational speeds**

Tool speed, mm/min	T-statistic	Conclusion
80	3.67	Since $3.67 < \chi_{(0.05,3)}^2(=7.81)$, do not reject the null-hypothesis
95	7.76	Since $7.76 < \chi_{(0.05,3)}^2(=7.81)$, do not reject the null-hypothesis
130	4.33	Since $4.33 < \chi_{(0.05,3)}^2(=7.81)$, do not reject the null-hypothesis
200	6.76	Since $6.76 < \chi_{(0.05,3)}^2(=7.81)$, do not reject the null-hypothesis

The results of the aforementioned procedure are summarized
 in Table 4. It is seen that the T -statistic values associated with the
 603 80, 95, 130, and 200 mm/min tool translational speeds, are
 604 3.67, 7.76, 4.33, and 6.76, respectively. Since all the four
 605 T -statistic values are smaller than the critical chi-square value,
 606 $\chi_{(0.05,3)}^2(=7.81)$, at a confidence level of 0.95, the null hypothesis
 607 defined earlier in this section cannot be rejected. To summarize,
 608 the results obtained in this section simply suggest that the
 609 surface condition of the fatigue specimen may not have a first-
 610 order effect on the FSW-joint fatigue strength/life in a range of
 611 weld-material microstructure, defect content, and properties
 612 brought about by a variation in the tool translational speeds
 613 between 80 and 200 mm/min. In other words, crack initiation
 614 occurring predominantly on the specimen surface may not have
 615 a dominant effect on the overall FSW-joint fatigue strength/life.

616 It should be recalled that all the fatigue data used in this
 617 study were obtained under uniaxial loading conditions under
 618 which stress distribution across the specimen cross-sectional
 619 area is uniform. Fatigue testing is often also carried out under
 620 cyclic bending/torsional loading conditions. In this case, the
 621 highest stresses are located in the surface regions of the tensile
 622 specimen and, hence, the role of surface condition can be
 623 expected to be more significant.

4. Summary and Conclusions

626 Based on the study reported and discussed in this article, the
 627 following main summary remarks and conclusions can be
 628 made:

629 1. Owing to intrinsic variability and stochastic nature of
 630 the workpiece material microstructure/properties, the use
 631



632 of statistical methods and tools in the analysis of friction
 633 stir welding (FSW) joints is highly critical. This is
 634 particularly the case when one deals with fatigue strength
 635 and life properties of these joints since these properties
 636 are highly affected by the material microstructure and
 637 defect content as well as by the surface condition of the
 638 welds.

639 2. A three-step FSW-joint fatigue-strength/life statistical-
 640 analysis procedure is proposed in this study. Within this
 641 procedure, the type of the most appropriate probability
 642 distribution function is first identified. Then, the parameters
 643 of the selected probability distribution function are
 644 computed along with their confidence limits. Finally, the
 645 statistical significance of the effect of the variates (the
 646 tool translational speed and the fatigue-specimen surface
 647 condition) is assessed.

648 3. This procedure showed that, within their respective
 649 ranges of variation, while the tool translational speed has
 650 a first-order effect on the FSW-joint fatigue strength/life,
 651 the effect of the fatigue specimen surface condition is
 652 less pronounced.

653 **Acknowledgments**

654 The material presented in this article is based on study
 655 supported by the U.S. Army/Clemson University Cooperative
 656 Agreements W911NF-04-2-0024 and W911NF-06-2-0042, and
 657 by the Army Research Office-sponsored grant W911NF-09-1-
 658 0513.

References

1. W.M. Thomas, E.D. Nicholas, J.C. Needham, M.G. Murch, P. Temple-Smith, and C.J. Dawes, Friction Stir Butt Welding, International Patent Application No. PCT/GB92/02203, 1991
2. M. Grujicic, G. Arakere, H.V. Yalavarthy, T. He, C.-F.Yen, and B.A. Cheeseman, Modeling of AA5083 Material-microstructure Evolution during Butt Friction-stir Welding, *J. Mater. Eng. Perform.*, 2009, doi:10.1007/s11665-009-9536-1
3. M. Grujicic, T. He, G. Arakere, H.V. Yalavarthy, C.-F.Yen, and B.A. Cheeseman, Fully-Coupled Thermo-Mechanical Finite-Element Investigation of Material Evolution during Friction-Stir Welding of AA5083, *J. Eng. Manuf.*, 2009. doi:10.1243/09544054JEM1750
4. M. Grujicic, G. Arakere, B. Pandurangan, A. Hariharan, C.-F.Yen, and B.A. Cheeseman, Development of a Robust and Cost-Effective Friction Stir Welding Process for Use in Advanced Military Vehicle Structures, *J. Mater. Eng. Perform.*, submitted April 2010
5. *Armor Plate, Aluminum Alloy, Weldable 5083 and 5456*; MIL-DTL-46027J, U.S. Department of Defense, Washington, DC, August 1992
6. M.N. James, D.G. Hattingh, and G.R. Bradley, Weld Tool Travel Speed Effects on Fatigue Life of Friction Stir Welds in 5083 Aluminum, *Int. J. Fatigue*, 2003, **25**, p 1389–1398
7. A. Lamarre and M. Moles, Ultrasound Phased Array Inspection Technology for the Evaluation of Friction Stir Welds, *Proceedings of the 15th World Conference on Nondestructive Testing*, Rome, Italy; Brescia, Italy, October 2000
8. R.B. D'Agostino and M.A. Stephens, *Goodness-of-Fit Technique*, Dekker, New York, 1986
9. L. Goglio and M. Rossetto, Comparison of Fatigue Data Using the Maximum Likelihood Method, *Eng. Fract. Mech.*, 2004, **71**, p 725–736
10. W. Nelson, *Applied Life Data Analysis*, John Wiley & Sons, 1982
11. R.A. Fisher, *Statistical Methods for Research Workers*, Oliver & Boyd, Edinburgh, 1925
12. G. Minak, L. Ceschinini, I. Boromei, and M. Ponte, Fatigue Properties of Friction Stir Welded Particulate Reinforced Aluminum Matrix Composites, *Int. J. Fract.*, 2010, **32**, p 218–226

659 660 661 662 663 664 665 666 667 668 669 670 671 672 673 674 675 676 677 678 679 680 681 682 683 684 685 686 687 688 689 690 691 692 693 694